



TITLE:

Multiple K-shell excitation of lithium clusters: Implications for hollow-atom solids

AUTHOR(S):

Kitamura, Hikaru

CITATION:

Kitamura, Hikaru. Multiple K-shell excitation of lithium clusters: Implications for hollow-atom solids. Chemical Physics Letters 2009, 475(4-6): 227-231

ISSUE DATE:

2009-06

URL:

<http://hdl.handle.net/2433/84950>

RIGHT:

Copyright © 2009 Elsevier B.V.; この論文は出版社版ではありません。引用の際には出版社版をご確認ご利用ください。 ; This is not the published version. Please cite only the published version.

Multiple K-shell excitation of lithium clusters: Implications for hollow-atom solids

Hikaru Kitamura*

Department of Physics, Kyoto University, Sakyo-ku, Kyoto 606-8502, Japan

Abstract

Systematic molecular-orbital calculations are performed for Li_9^{z+} clusters in which N_{exc} ($= 0-9$) core electrons are excited to valence orbitals. For neutral ($z=0$) clusters, the magnitudes of work functions, cohesive energies, and average core-electron excitation energies *increase* with N_{exc} , owing to relaxation of valence electrons around localized core holes. Total energy of a multiply charge ion, produced by a series of Auger decay, remains lower than the corresponding dissociation limit as far as $z \leq 3$. We thereby discuss a possibility of realizing a *hollow-atom solid*, multiply core-excited state with temporal crystalline order, by utilizing intense free-electron lasers.

* E-mail: kitamura@scphys.kyoto-u.ac.jp

1. Introduction

Recent development of free-electron laser (FEL) technologies is opening up a possibility of coherent laser light in the vacuum ultraviolet (VUV) and X-ray regions with significantly small energy dispersions [1-3]. When a solid target is irradiated by an intense ultra-short FEL pulse with its photon energy matching the absorption edge, it is possible in principle to excite many core electrons to the valence or conduction band slightly above the Fermi level while the lattice structure remains transiently undestroyed. Such a multiply core-excited crystalline state may be called a *hollow-atom solid* [4] by analogy with the familiar isolated hollow atoms [5]. The hollow-atom solid bears a resemblance to the dense electron-hole liquid in photoexcited semiconductors [6], though the lifetime of the former is expected to be smaller due to the Auger decay.

The laser intensity I required to realize a hollow-atom solid with one core hole per atom may be estimated roughly as $I \cong E_{\text{edge}} / \sigma_{\text{edge}} \Delta t$, where σ_{edge} denotes the photoabsorption cross section per atom at the edge energy E_{edge} , and Δt is the laser pulse width. For K-shell excitation of a lithium crystal with a laser pulse of $\Delta t \cong 100$ fs, we substitute $E_{\text{edge}} \cong 55$ eV and $\sigma_{\text{edge}} \cong 3 \times 10^{-18}$ cm²/atom [7] to obtain $I \cong 2.9 \times 10^{13}$ W/cm², which may be attainable with VUV FEL.

Laboratory demonstration of a hollow-atom solid is an important and challenging subject from the viewpoints of both fundamental physics and technological applications. Because the inner-shell vacancies strongly perturb the surrounding electrons, the absorption edge energy would shift during the multiple excitation process; if the edge shifts toward higher energies, the absorption coefficient at the original edge will suddenly decrease and hence the system may act as a saturable absorber switch for X-rays [4]. We also point out that achievement of population inversion in hollow-atom solids may lead to gain on stimulated free-bound emission [8].

Collisional radiative processes in laser-produced photoionized plasmas are often analyzed by assuming classical statistics for free electrons and atomic models for bound-state energy levels [8]. In low-temperature hollow-atom solids, we encounter additional complications stemming from energy-band structures due to the overlap of adjacent atomic

wavefunctions and Fermi degeneracy of conduction electrons. Moreover, the response of electrons to multiple core holes is difficult to analyze for a real material, although a formal many-body theory exists [9].

In this Letter, we present quantum-chemical LCAO-MO analysis of multiply core-excited Li_9 clusters as prototypical models of hollow-atom solids, and investigate how the presence of multiple core holes affects their electronic structures and stabilities. Although the cluster size is too small to reproduce bulk properties exactly, the present model facilitates quantitative and systematic investigations of many-electron relaxation effects and cohesive properties for various core-hole configurations and charge states. Cluster models are especially useful to describe symmetry breaking associated with core-hole localization, which cannot be expressed easily in terms of periodic Bloch wavefunctions.

2. Method of calculation

We study Li_9^{z+} clusters with various core-hole configurations illustrated in Fig. 1. The cluster geometry is fixed at a body-centered cubic (bcc) configuration, which corresponds to the stable lattice structure of bulk lithium at room temperature [10]. Each excited state is characterized by the parameters N_{exc} and z denoting the number of excited 1s electrons (i.e., the number of core holes) and net charge of the cluster, respectively. Hereafter, the nearest-neighbor separation R_{nn} is fixed at the bulk lattice constant, $R_{\text{nn}}=5.7$ a.u. [10], because the nuclei will not move appreciably within a subpicosecond timescale comparable to Δt .

The electronic structures of the clusters are studied through all-electron LCAO-MO calculations based on the unrestricted Hartree-Fock (UHF) method [11], an approximate but useful tool to analyze excited states of general open-shell systems. The many-body wave function is approximated by a single Slater determinant of the form, $\Psi = \left| \psi_1^\alpha \cdots \psi_{N_e^\alpha}^\alpha \psi_1^\beta \cdots \psi_{N_e^\beta}^\beta \right|$, where the total numbers of up-spin (α) and down-spin (β) electrons are denoted as N_e^α and N_e^β , respectively. The one-electron orbital wave functions $\psi_k^\alpha(\mathbf{r})$ and $\psi_k^\beta(\mathbf{r})$ with MO index k are expanded in terms of Slater-type orbitals (STOs) [11]

centered at each atomic site; they consist of 1s ($\zeta = 4.62, 2.46$), 2s ($\zeta = 1.96, 0.672$), and $2p_{x,y,z}$ ($\zeta = 1.96, 0.672$) functions, where the values of the radial exponent ζ have been taken from atomic data [12]. The use of such double-zeta basis sets is necessary to allow for large modification of electron distribution around core holes. In our computational code, the one- and two-center integrals involving electron kinetic energy, electron-electron and electron-nucleus interactions are evaluated with analytic formulas [13], while other non-analytic integrals are evaluated within the STO-3G approximations [14].

An excited state with given N_{exc} and z can be described by Ψ in which N_{exc} core electrons are transferred to the lowest unoccupied valence MOs, with z electrons being further removed from the valence MOs. Self-consistent iterative solutions to the resultant Pople-Nesbet equations [11] converge to a state in which all the core holes are localized at around atomic sites and surrounding electrons are fully relaxed; the MO energy levels $\varepsilon_k^\alpha, \varepsilon_k^\beta$ and the corresponding wavefunctions are thus obtained. To achieve convergence for a neutral excited state, we have adopted wavefunctions of a positive ion with the same N_{exc} -value as an initial input to the iteration.

3. Results and discussion

3.1. Test calculations for a dimer

To check the numerical accuracy of the present UHF method, we have calculated potential energy curves of a Li_2 dimer in the ground ($X^1\Sigma_g^+$) and core-excited ($^1\Sigma_u^+, ^1\Sigma_g^+$) states, which are compared with the configuration-interaction (CI) calculations by Schwarz *et al* [15] in Fig. 2. The CI calculation predicts total energies lower than those of the UHF theory because of the electron correlation effects included in the former. Apart from the constant energy difference, however, the overall shapes of the CI and UHF curves are similar. Accordingly, we will mainly discuss cohesive energies rather than total energies in subsequent sections to reduce an error inherent in the UHF approximation. We note that the neutral doubly excited $^1\Sigma_g^+$ state, correlating to the $\text{Li}^*(1s2s^2)\text{-Li}^*(1s2s^2)$ asymptote, exhibits a clear bound state; the corresponding CI data have not been reported so far.

3.2. Electronic structures

Figure 3 displays occupied MO energy levels for neutral Li_9 clusters, which clearly indicates the importance of many-body effects: excitation of one core electron modifies the entire electronic structure of a cluster. Our previous paper [16] has reported only results for $N_{\text{exc}} \leq 2$, whereas the present work contains complete data up to $N_{\text{exc}} = 9$ corresponding to the hollow-atom solid. Salient features are summarized as follows:

(i) The core levels are split into upper and lower sublevels. In the ground state, each atomic 1s orbital is doubly occupied, which constitutes the upper sublevels. When one electron is removed, the remaining electron (having opposite spin) in the same orbital is strongly attracted by the nuclear Coulomb field, which is responsible for the lower sublevels. In the near-edge photoabsorption, core excitation occurs from the upper sublevels until they disappear when N_{exc} reaches 9.

(ii) The bottom of the valence MO is lowered as N_{exc} increases, which reveals that the valence electrons are strongly attracted by the localized core holes.

(iii) The work function W , estimated as a minus of the energy of the highest occupied MO, *increases* from 3.35 eV to 7.14 eV as N_{exc} varies from 0 to 9. This nontrivial feature arises as a consequence of downward shift of the entire valence levels due to the core-hole screening despite the fact that more electrons populate in higher MO levels as excitation proceeds. We note that, for the ground state, the previous UHF calculation by Marshall *et al* [17] using Gaussian basis sets predicted $W = 3.41$ eV, which is in good agreement with the present result (3.35 eV). For a comparison, the experimental value of W for bulk crystal amounts to 2.9 eV [18].

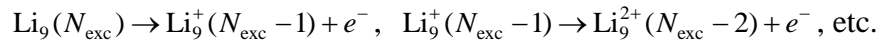
3.3 Cohesive energies

In order for a stable operation of hollow-atom solid as an optical device, it is desirable that the crystalline order and the electronic band structure are not immediately destroyed. The lattice stability of a Li_9^{z+} cluster may be measured by the cohesive energy, $E_{\text{coh}} = E - E(R_{\text{nn}} \rightarrow \infty)$, defined as the total energy E relative to the dissociation limit, $E(R_{\text{nn}} \rightarrow \infty) \equiv (N - N_{\text{exc}} - z)E(\text{Li}) + N_{\text{exc}}E(\text{Li}^*) + zE(\text{Li}^+)$. Here, $E(\text{Li}) = -7.4327$ a.u., $E(\text{Li}^*)$

= -5.3284 a.u., and $E(\text{Li}^+) = -7.2364$ a.u. correspond the energy of atomic $\text{Li}(1s^2 2s)$, $\text{Li}^*(1s 2s^2)$, and $\text{Li}^+(1s^2)$ states, respectively, in the present UHF calculation; $N = 9$ is the cluster size.

The computed values of E_{coh}/N are plotted in Fig. 4 for various combinations of N_{exc} and z . We find that the neutral ($z=0$) core-excited clusters have negative E_{coh} over the entire range of N_{exc} and hence they are stable against dissociation. The value of E_{coh}/N decreases from -0.31 eV/atom to -1.00 eV/atom as N_{exc} increases from 0 to 9, indicating that the hollow-atom cluster ($N_{\text{exc}} = 9$) is particularly stable.

In reality, each core hole has a finite lifetime due to the KVV Auger decay [9] accompanying emission of a valence electron. Hence, the neutral core-excited cluster should eventually be multiply ionized through the reactions,



Almbladh et al. [19] estimated the Auger decay lifetime of a single core hole, τ_0 , in bulk lithium metal as $\tau_0 \approx 40$ fs, though it is sensitive to the treatment of orbital relaxation and the wavefunction of the outgoing electron. When multiple core holes exist, the time for *either* one of the core holes to decay becomes smaller than τ_0 , as we shall discuss later in the next section. It can be seen in Fig. 4, however, that singly ($z = 1$) and doubly ($z = 2$) charged ions still have negative cohesive energies comparable to neutral clusters, suggesting that dissociation (i.e., Coulomb explosion [20,21]) may not be triggered during such an early stage of multiple Auger decay. Since the cohesive force in a metal stems predominantly from delocalized valence electrons, further loss of valence electrons causes weakening of the bonding. Indeed, E_{coh} reaches nearly zero for $z = 3$ and then turns into large positive values for $z \geq 4$. We thus estimate the condition for the onset of Coulomb explosion as $z/N > 3/9 = 0.33$.

In Fig. 4, the curve labeled as $z = N_{\text{exc}}$ represents the case where the core electrons are immediately ionized above the vacuum level. Those ions become highly unstable once N_{exc} exceeds 3, in contrast to the stability of neutral excited states that persists up to $N_{\text{exc}} = 9$. Thus, we should excite electrons below the vacuum level in order to delay the onset of Coulomb explosion.

3.4 Core-electron excitation energies

We plot in Fig. 5 a core-electron excitation energy, $E_{\text{exc}} = E - E(N_{\text{exc}}=z=0)$, required to achieve a multiple core-excited state with given N_{exc} and z from the initial ground state. We find that the quantity $E_{\text{exc}}/N_{\text{exc}}$ evaluated at $z = 0$ (i.e., neutral excitation) increases by about 1 eV as N_{exc} increases from 1 to 9. This means that the K-shell photoabsorption edge undergoes a blue shift as multiple excitation proceeds. Here, the identification of $E_{\text{exc}}/N_{\text{exc}}$ as the absorption edge may be validated since the mixing of valence 2s and 2p states in a cluster makes the dipole oscillator strengths of any core-valence transition finite and hence the absorption edge is given simply as a minimum energy difference before and after a core-hole creation. We note that the experimentally measured K-edge of bulk lithium metal is 54.7 eV [22], which compares with our cluster calculation, 55.7 eV.

Analogous quantity, $E_{\text{exc}}/N_{\text{exc}}$ at $z = N_{\text{exc}}$, represents an average core-ionization energy needed to create a $\text{Li}_9^{N_{\text{exc}}+}$ cluster. Steep increase of this quantity as a function of N_{exc} reveals that considerable amount of additional energy is required to ionize a core electron when multiple core holes are already present.

4. Implications for hollow-atom solids

In summary, we have presented a systematic LCAO-MO analysis of multiply core-excited lithium clusters for various combinations of N_{exc} (number of core holes) and z (net cluster charge) by taking into account many-electron relaxation effects within the UHF approximation. In light of the electronic structures and cohesive energies so obtained, we draw the following conclusions concerning a possible formation of hollow-atom solids.

(i) If we can excite many core electrons rapidly to the conduction band below the vacuum level, strong attractive potentials are created at around localized core holes and they prevent excited electrons from immediate ionization. An intense FEL pulse with sufficiently small energy dispersion must be used for this purpose. The resultant *neutral* excited state is shown to be stable for the entire range of $N_{\text{exc}} \leq N$, with N denoting the total number of atoms, in a sense that the magnitudes of cohesive energies and work functions are both large.

(ii) The neutral hollow-atom solid eventually undergoes multiple valence ionization due to Auger decay. The present cluster calculation reveals that the cohesive energy changes sign at $z/N > 3/9 = 0.33$, indicating an onset of Coulomb explosion. The onset time τ of Coulomb explosion for a neutral hollow-atom solid with N_{exc} initial core holes may be estimated as follows: Since the core holes are strongly localized and separated from each other, we may assume in a first approximation that they decay independently with a lifetime τ_0 (≈ 40 fs for lithium [19]) appropriate to a single core hole. Supposing that Auger decays occur z times during time τ , we arrive at a relation $N_{\text{exc}} - z = N_{\text{exc}} \exp(-\tau/\tau_0)$, which yields

$$\tau = \tau_0 \ln \frac{1}{1 - (z / N_{\text{exc}})} = \tau_0 \ln \frac{1}{1 - 0.33(N / N_{\text{exc}})}. \quad (1)$$

Thus, the onset time of dissociation becomes shorter as the initial N_{exc} becomes larger: In the limiting case $N_{\text{exc}}=N$, we obtain $\tau \approx 0.40 \tau_0 \approx 16$ fs. It remains to be seen how interatomic effects stemming from neighboring core holes may alter the lifetime through modification of the incoming and outgoing electron wavefunctions that enter the Auger matrix element [23]. We note that different onset values of z/N or τ may be predicted for other heavy elements, for which Auger electrons are emitted from inner shells rather than valence orbitals.

(iii) The threshold energy of core-electron excitation turns out to be an increasing function of N_{exc} , with a total increment of about 1 eV as N_{exc}/N varies from 0 to 1. If such an excitation-energy shift causes abrupt reduction of absorption cross section in the course of laser irradiation, we may expect saturation of absorption, though detailed computation of absorption spectra is needed to confirm such a possibility.

Finally, we remark that complete assessment of the experimental feasibility of hollow-atom solids still await for improved and advanced analyses, as we mention in the following:

(a) The discrepancy between the cohesive energies of Li_9 (-0.31 eV/atom) and bulk Li metal (-1.6 eV/atom) [10] in the ground state exposes a smallness of cluster size in the present work. A large-cluster calculation might modify the critical ionization degree z/N , which affects the onset time τ of Coulomb explosion through Eq. (1). The influence of electron correlation in the cohesive energies should also be investigated.

(b) In photoabsorption experiments, core electrons are generally excited to higher

valence levels. The whole manifold of higher MOs can be computed with the aid of the improved virtual orbital method [24] once we have obtained the data on fully relaxed core-hole states in this work. For elucidation of subsequent electron relaxation process, those MO levels and wavefunctions should be incorporated into the quantum collisional equations for the electrons [25,26]. During relaxation, excess electron energies can be transferred to ions as well; the resultant phonon excitation [26] is overlooked in the present static analysis.

(c) An outgoing electron in the Auger decay has a large kinetic energy, which could contribute to heating in the valence band.

Acknowledgments

The author is grateful to Dr. K. Nagaya and Dr. H. Yoneda for pertinent discussions. This work was supported in part through Grant-in-Aid for Promotion of Utilization of X-Ray Free-Electron Lasers provided by the Japanese Ministry of Education, Science, Sports and Culture.

References

- [1] T. Shintake et al, *Nature Photonics* 2 (2008) 555.
- [2] W. Ackermann et al, *Nature Photonics* 1 (2007) 336.
- [3] J. Arthur, *Rev. Sci. Instrum.* 73 (2002) 1395.
- [4] H. Yoneda, Private communication.
- [5] H. Winter, F. Aumayr, *J. Phys. B: At. Mol. Opt. Phys.* 32 (1999) R39.
- [6] M. Nagai, R. Shimano, K. Horiuchi, M. Kuwata-Gonokami, *Phys. Stat. Sol. (b)* 238 (2003) 509.
- [7] C.T. Chantler, *J. Phys. Chem. Ref. Data* 24 (1995) 71.
- [8] R. Kodama, *Phys. Rev. Lett.* 69 (1992) 77.
- [9] L.S. Cederbaum, *Phys. Rev. A* 35 (1987) 622.
- [10] D.A. Young, *Phase Diagrams of the Elements*, Univ. California Press, 1991, Chap. 5 and Appendixes.
- [11] A. Szabo, N.S. Ostlund, *Modern Quantum Chemistry: Introduction to Advanced Electronic Structure Theory*, Macmillan, 1982, Chap. 2 and 3.
- [12] E. Clementi, C. Roetti, *At. Data Nucl. Data Tables* 14 (1974) 177.
- [13] C.C.J. Roothaan, *J. Chem. Phys.* 19 (1951) 1445.
- [14] P. Montagnani, O. Salvetti, *Int. J. Quant. Chem.* 43 (1992) 273.
- [15] W.H.E. Schwarz, W. Butscher, D.L. Ederer, T.B. Lucatorto, B. Ziegenbein, W. Mehlhorn, H. Prömpeler, *J. Phys. B: Atom. Molec. Phys.* 11 (1978) 591.
- [16] H. Kitamura, *Eur. Phys. J. D* 52 (2009) 147.
- [17] R.F. Marshall, R.J. Blint, A.B. Kunz, *Phys. Rev. B* 13 (1976) 3333.
- [18] D.R. Lide (Ed.), *CRC Handbook of Chemistry and Physics*, 72th Ed., CRC Press, 1991, Sec. 12-97.
- [19] C.-O. Almbladh, A.L. Morale, G. Grossmann, *Phys. Rev. B* 39 (1989) 3489.
- [20] E. Rühl, 2003 *Int. J. Mass Spectrom.* 229 (2003) 117.
- [21] S.P. Hau-Riege, R.A. London, A. Szoke, *Phys. Rev. E* 69 (2004) 051906.
- [22] P. Haensel, G. Keitel, B. Sonntag, C. Kunz, P. Scheriber, *Phys. Stat. Sol. (a)* 2 (1970) 85.

- [23] F.P. Larkins, J. Elec. Spectr. Rel. Phenomena 51 (1990) 115.
- [24] W.J. Hunt, W.A. Goddard III, Chem. Phys. Lett. 3 (1969) 414.
- [25] P.M. Echenique, J.NM. Pitarke, E.V. Chulkov, A. Rubio, Chem. Phys. 251 (2000) 1.
- [26] N. Del Fatti, C. Voisin, M. Achermann, S. Tzortzakis, D. Christofilos, F. Vallee, Phys. Rev. B 61 (2000) 16956.

Figure captions

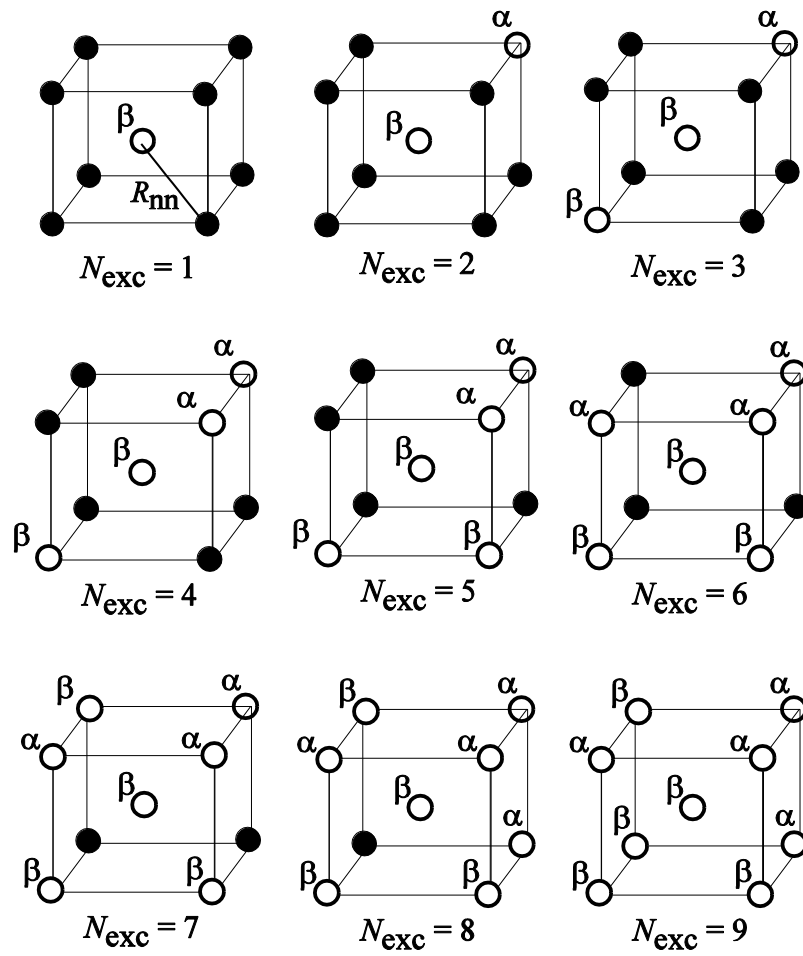
Fig. 1. Atomic configurations of Li_9 clusters in the core-excited states. The white circles designate the positions of core holes, with a corresponding spin index α or β of the excited electron.

Fig. 2. Total energy of a Li_2 dimer as a function of the internuclear distance. The solid curves represent the present calculations; the dashed curves depict the CI calculations by Schwarz et al [15]. The corresponding energies in the dissociation limit are indicated at the right edge of each column.

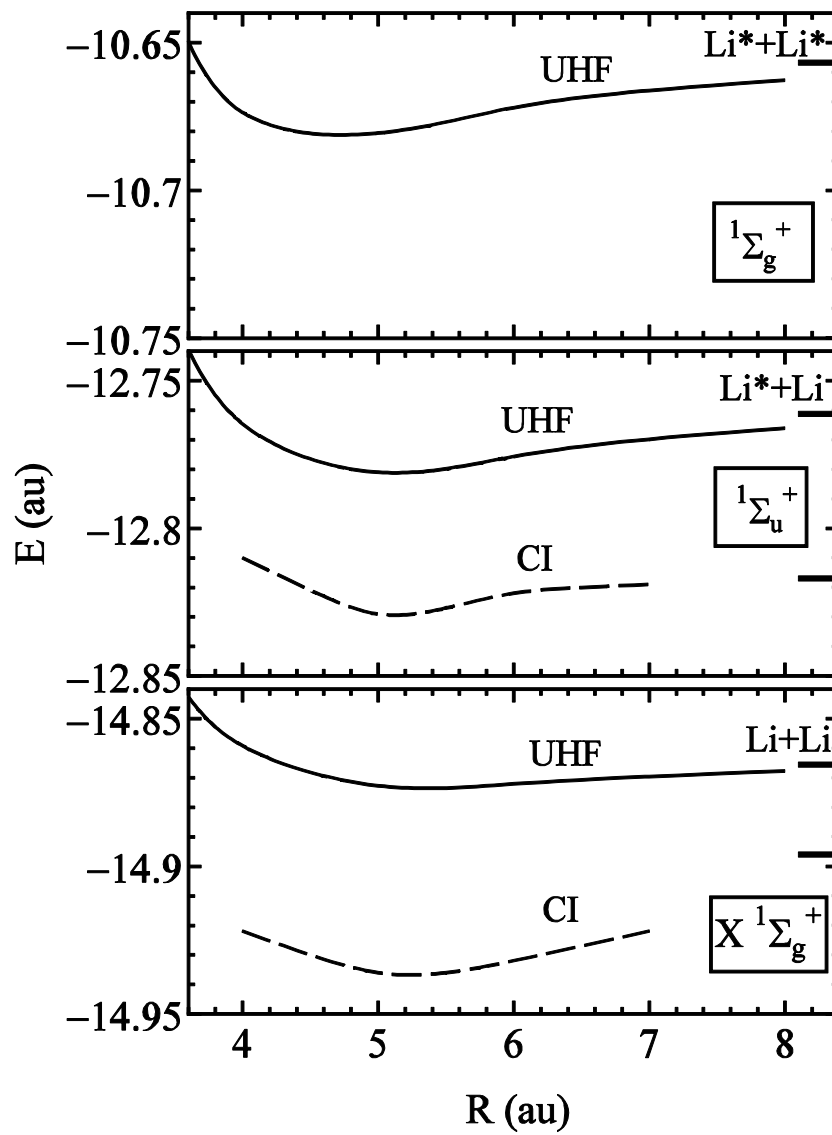
Fig. 3. Occupied MO levels of core-excited neutral Li_9 clusters with $R_{\text{nn}}=5.7$ a.u. The upper and lower panels correspond to valence and core states, respectively.

Fig. 4. Cohesive energies of core-excited Li_9^{z+} clusters with $R_{\text{nn}}=5.7$ a.u.

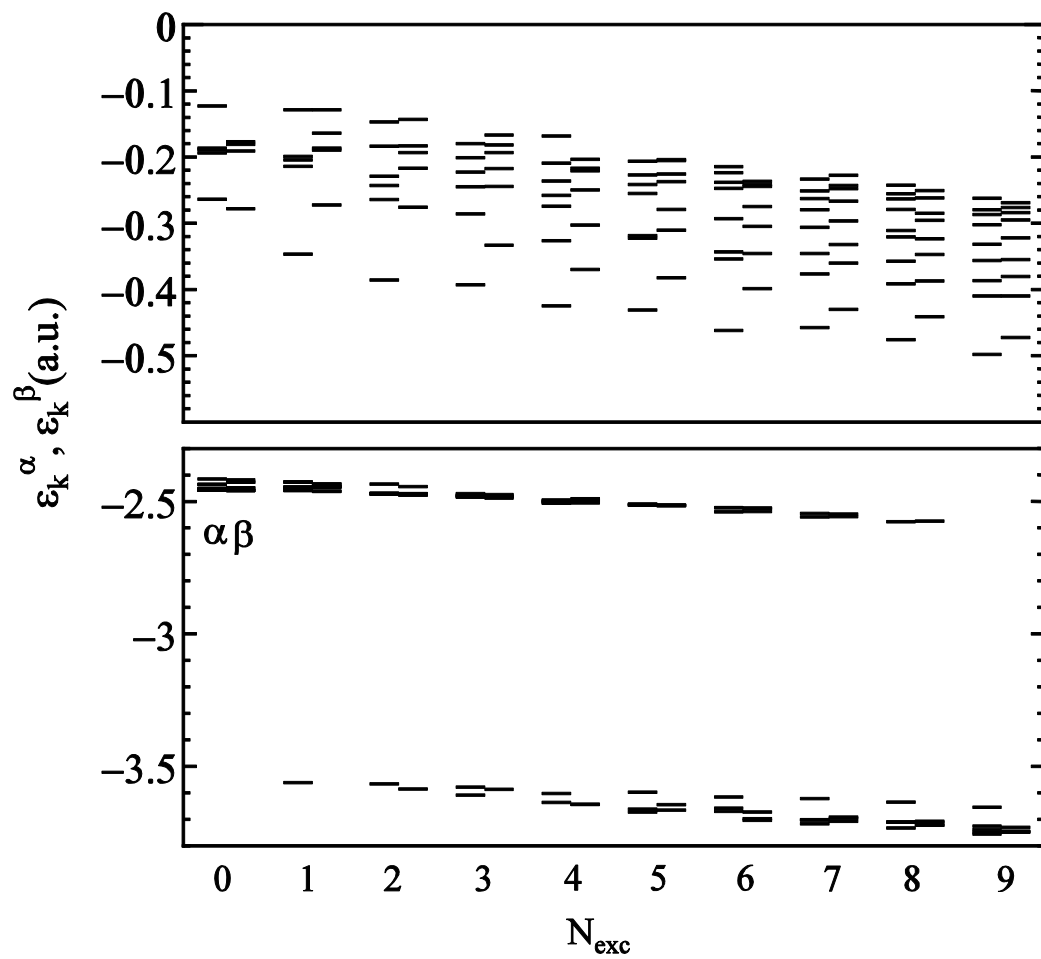
Fig. 5. Average core-electron excitation energies to create Li_9^{z+} clusters with N_{exc} core holes from the ground state.



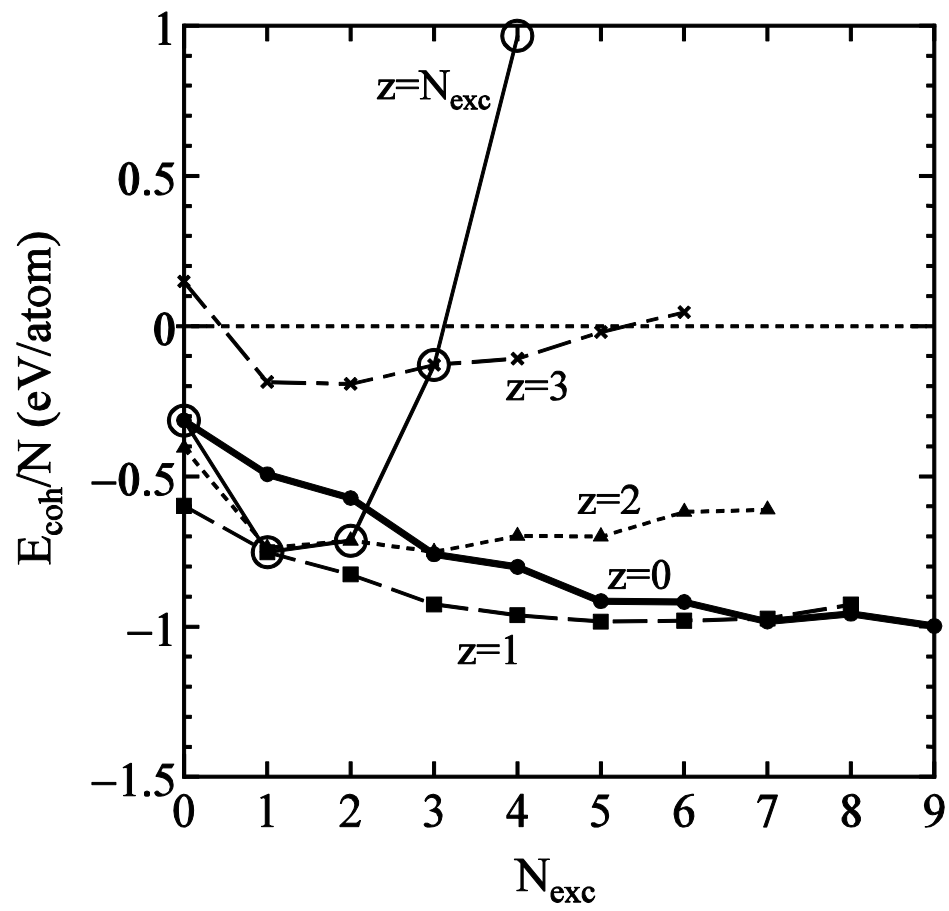
Kitamura Fig. 1



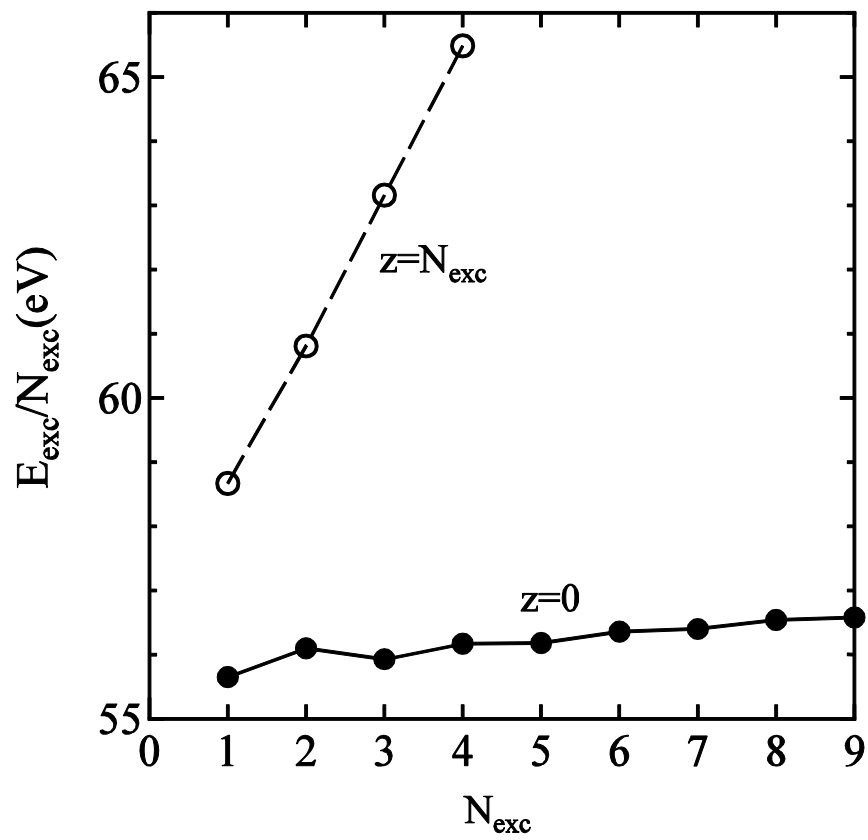
Kitamura Fig. 2



Kitamura Fig. 3



Kitamura Fig. 4



Kitamura Fig. 5